콘크리트의 균열개구 변위와 하중방향 변위 관계

Relationship between the CMOD and the Load - Line Deflection of Concrete

김석기*

Kim, Suk Ki

요 약

통상적인 방법에 의해 측정된 콘크리트 보의 변위는 지지점의 국부변위나 변위의 측정 위치에 따른 외부적인 요인이 포함된다. 이러한 오류에 의한 변위의 크기는 실제 변위크기와 거의 같은 정도이기 때문에 이를 사용하여 정확한 파괴 파라메타를 구하기 어렵다. 본 연구에서는 외부적인 요인의 영향을 받지 않는 균열개구 변위와 하중작용 방향 변위의 상관관계를 규명하고, 하중 개구부 변위를 파괴특성을 구하는 인자로 사용하였다. 균열개구 변위와 하중방향 변위는 서로 비례함을 알 수 있었으며, 이 비례관계를 이용하여 RILEM에서 제시한 파괴에너지 결정방법에 대한 문제점을 발견하였고 이에 대한 수정방법을 제시하였다.

Abstract

Traditional displacement measurement included an extraneous and erratic portion due to test setup and support crushing. The magnitude of this erroneous deformation was

* 정회원, 단국대학교 공학대학 토목공학과 부교수

• 본 논문에 대한 토의를 1997년 4월 30일까지 학회로 보내주시면 1997년 6월호에 토의회답을 게재하겠습니다.

found to be of the same order as the actual displacement, leading to inaccurate determinations of fracture parameters. To overcome this problem, the load-*CMOD* relationship is a more reliable parameter for determining the fracture characteristics because it is unaffected by the specimen setup and any support crushing.

An important step towards the use of load-CMOD concept as a key fracture parameter depends on relating the *CMOD*to the traditional load-line deflection. This investigation found that there was an unique linear relationship between the *CMOD* and the load-line deflection. The exact numeric value of relationship between the *CMOD* and the deflection, that is, the slope of the line, is discovered to be a material property. The relationship finds a problem with the existing RILEM recommendations for measuring the fracture energy of concrete. A proposal to correct the problem is made.

Keywords : load - *CMOD* relationship, load-line deflection, fracture energy, support crushing

1. Introduction

Due to concrete's low tension resistance, most of the failures observed in concrete structures are initiated by local tensile failure in an area of high stress concentrations or within a zone of pre-existing flaws. Recently, it has been realized that in order to improve the serviceability and safety of concrete structures, the tensile fracture resistance of concrete has to be incorporated into the analysis procedures.[1,2,3]

Important fracture parameter is the fracture energy (G_F), which has a physical meaning similar to the critical strain energy release rate, and is determined from the work needed to completely separate a specimen into two halves. The real value of G_F is obtained from a direct tensile test. Because of the difficulties involved in performing the direct uniaxial tensile test, three-point bend tests on notched beams were suggested from the International Union of Testing and Research Laboratories for Materials and Structures (RILEM) for determining the fracture energy.[4] The energy consumed during fracture is a direct function of the load-displacement response. The traditional displacement measurement includes extraneous deformation due to test setup and supports crushing. Unfortunately, the magnitude of this erroneous deformation was found to be of the same order as the actual displacement, leading to inaccurate fracture parameters.[5,6] To overcome this problem, the load-crack mouth opening displacement (load-*CMOD*) relationship is a more reliable parameter unaffected by the specimen setup and any support crushing.

The *CMOD* has primarily been used in closed-loop testing as the control parameter to ensure a stable failure of specimen so that the fracturing activities around the peak load and through the post-peak regions can be clearly observed. However, since the *CMOD* is unaffected by support settlement it is thought that it might be a more reliable fracture parameter.

This investigation found that there is an unique linear relationship between the *CMOD* and the load-line deflection, provided that deflection is measured accurately. The numeric value of the relationship between *CMOD* and the load-line deflection ,that is, the slope of the line, is shown to be a material property. With the proposed relationship, existing RILEM recommendations for measuring the fracture energy of concrete will have to be modified.

An experimental program is undertaken to examine the relationship between the *CMOD* and load-line deflection. Three different specimen sizes and four different notch depths for each size are evaluated in the three-point bend notched beam test.

The load, *CMOD*, load-line deflection measured with reference to the neutral axis of the beam, and load-line deflection with reference off the beam (traditional displacement measurement) are monitored to check and investigate the fracture parameters.

2. Analytical study

A load-displacement curve obtained from a displacement controlled test up to failure has two distinct regions : an ascending branch before, and a descending, softening branch after the peak load. The modulus of elasticity is usually used to characterize the stress-strain relation in the elastic domain, and the peak stress characterizes the tensile strength of an elastic material. However, in the process zone, it has been postulated, after analysis of the softening branch of uniaxial tension test results, that stress and the process zone displacements are functionally dependent through a local, process zone softening constitutive relation. The material in the process zone supports stresses after the peak load which is proportional to the displacement in the process zone. One constitutive relation holds between stress-strain in the elastic domain, e.g., modulus of elasticity, and another holds between stress and process zone displacements in the process zone.

2.1 Linear elastic range

For the initial portion, the linear elastic range, the linear elastic fracture mechanics concept can be used to obtain a *CMOD* - load-line deflection. Crack mouth opening displacement is

$$CMOD = \frac{6Psa}{Ebd^2} V_1(A) = \frac{6Ps}{Ebd} AV_1(A) \quad (1)$$

where P is the load, s, the span of the beam, b, the beam width, d, the beam deptht, a, the initial notch depth. A is the ratio of the initial notch depth to beam depth (a/d) and $V_1(A)$ is a correction factor[7] dependent on the loading type and the ratio of the span to the beam depth. In the case of the three-point bend test specimen for s/d = 4, $V_1(A)$ is

$$V_1(A) = 0.76 - 2.28A + 3.87A^2 - 2.04A^3 + \frac{0.66}{(1-A)^2} \quad (2)$$

The total load-line deflection of beam δ_p can be expressed as

$$\delta_p = \delta_c + \delta_u = \delta_c + (\delta_b + \delta_s) \quad (3)$$

where δ_c is the deflection due to the

crack[7], δ_u is the deflection of the uncracked beam, δ_b is the deflection due to bending and δ_s is the deflection due to shear.

$$\delta_b = \frac{Ps^3}{4Ebd^3}$$

$$\delta_s = \frac{3(1+\nu)Ps}{5Ebd} \tag{4}$$

$$\delta_c = \frac{3Ps^2}{2Ebd^2} V_2(A)$$

where

$$V_2(A) = \left(\frac{A}{1-A}\right)^2 (5.58 - 19.57A + 36.82A^2 - 34.94A^3 + 12.77A^4)$$

Substituting Eq. 4 into Eq. 3 and dividing by Eq. 1 gives

$$\frac{\delta_P}{CMOD} = \frac{30dsV_2(A) + 5s^2 + 12(1+\nu)d^2}{120daV_1(A)} \tag{5}$$

The value of $\nu = 0.2$ is commonly used for concrete and other cementitious materials. The derived formula should leave s/d as a variable but substitute the value of $\nu = 0.2$. Hence

$$\frac{\delta_P}{CMOD} = \frac{30(s/d)V_2(A) + 5(s/d)^2 + 14.4}{120AV_1(A)} \tag{6}$$

If s/d = 4 as recommended by ASTM standard[5], Eq. 6 is

$$\frac{\delta_P}{CMOD} = \frac{V_2(A)}{AV_1(A)} + \frac{23.6}{30AV_1(A)} \tag{7}$$

Based on the Eq. 5, load-line deflection can be expressed as follows :

$$\delta_P = S_1 \cdot CMOD$$

where S_1 is a constant determined by loading type and specimen geometry.

2.2 Post-peak range

To derive the relationship between *CMOD* and load-line deflection in post-peak range, following assumptions are used : (1) fracture energy, G_F, is a material property ; (2) microcracks are fully developed at the peak load, and when a crack propagates the size of fracture process zone does not change ; (3) the ratio of the change of *CMOD* to the change in crack length is constant (Fig. 1).

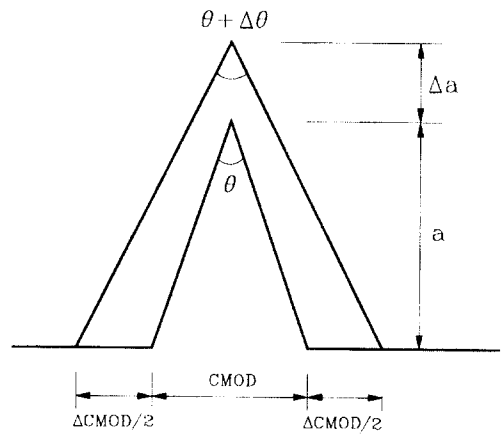

Fig. 1 Relation between *CMOD* and crack length *a*

The incremental ratio of load-line deflection to CMOD, $\Delta\delta_p / \Delta CMOD$, can be expressed using chain rule as

$$\frac{\Delta\delta_P}{\Delta CMOD} = \frac{\Delta a}{\Delta CMOD}\frac{\Delta\delta_P}{\Delta a} \tag{9}$$

The energy needed to produce a small increment of load-line deflection, ΔU is

$$\Delta U = P\,\Delta\delta_p \tag{10}$$

Substituting Eq. 10 into Eq. 9 gives

$$\frac{\Delta\delta_P}{\Delta CMOD} = \frac{\Delta a}{\Delta CMOD}\frac{\Delta U}{P\,\Delta a} \tag{11}$$

Since $\Delta U / \Delta a$ is the fracture energy G_F, Eq. 11 changes to Eq. 12.

$$\frac{\Delta\delta_P}{\Delta CMOD} = \frac{G_F}{bP}\frac{\Delta a}{\Delta CMOD} \tag{12}$$

The right side of above equation is a constant because G_F is a material property and $\Delta a / \Delta CMOD$ is a constant. Therefore, $\Delta\delta_P / \Delta CMOD$ is a constant.

$$\frac{\Delta\delta_P}{\Delta CMOD} = S_2 \tag{13}$$

S_2 is a material property, independent of size, and can be determined by experiments.

2.3 Microcracked process zone

In the microcracked process zone, microcracks start and fully develop at the peak load. Near the peak load, the coalescence of microcracks produces a traction-free surface in the process zone. This traction-free surface continuously changes causing a continuous slope change from S_1 to S_2 (Fig. 2).

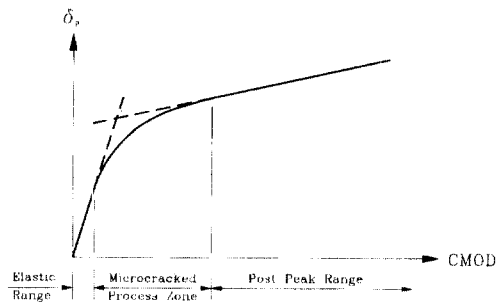

Fig. 2 δ_p--$CMOD$ curve

The change of slope, ΔS, due to increment of load ΔP is

$$\Delta S = \frac{\Delta\delta_P}{\Delta CMOD} = \frac{\frac{\partial\delta_P}{\partial a}\Delta a + \frac{\partial\delta_P}{\partial P}\Delta P}{\frac{\partial CMOD}{\partial a}\Delta a + \frac{\partial CMOD}{\partial P}\Delta P} \tag{14}$$

Rearranging the Eq. 14 with respect to P by using linear elastic fracture mechanics concept gives Eq. 15.

$$P = \frac{P_{max}}{1+K} \tag{15}$$

where

$$K = \frac{K_1\frac{3s^2}{2Ebd^3} - K_2\frac{6s}{Ebd^2}\Delta S}{\frac{\partial CMOD}{\partial P}\Delta S - \frac{\partial\delta_P}{\partial P}}\Delta a \tag{16}$$

$$K_1 = \left[2\frac{A}{(1-A)^3}(5.58 - 19.57A + 36.82A^2 - 34.94A^3 + 12.77A^4) + \left(\frac{A}{1-A}\right)^2(-19.57 + 73.64A - 104.82A^2 + 51.08A^3)\right] \tag{17}$$

$$K_2 = V_1(A) + A\left(-2.28 + 7.74A - 6.12A^2 + \frac{1.32}{(1-A)^3}\right) \tag{18}$$

Δa in Eq. 16 is calculated from the $CMOD$ value at the peak load using Eq. 1. Eq. 1 is a polynomial function of A requiring a numerical method for the determination of A. Since the effective crack length $a_e = a + \triangle a$, can be found. So, Eq. 15 can be solved for P, which is the proportional limit in this case.

3. Experimental program

Concrete mix-proportion, casting and curing procedure were kept constant for all specimens in order to minimize scatter by keeping the concrete as consistent as

possible for all samples. Ordinary portland cement was used with sand passing through sieve #4 and coarse basalt of 3/8 in. maximum size. Mix-proportion by weight is 1 : 2 : 2.5 (cement : sand : aggregate) with a water/cement ratio of 0.53.

ø3×6 in cylinder specimens were cast in disposable plastic molds to determine compressive strength and Young's modulus. The small and medium size beams were cast in plexy-glass molds and large size beams were cast in plywood molds. The beam dimensions are shown in Table 1.

Table 1 Size of specimens and number of specimens tested

Beam Size	Width(b) (inch)	Depth(d) (inch)	Length(L) (inch)	Span(s) (inch)	Weight (pound)
Small(S)	3	3	15	12	11.5
Medium(M)	3	4.5	21	18	24.3
Large(L)	3	6	27	24	42.1

Series	Notch depth / Beam depth(a/d)			
	0.2(N2)	0.33(N3)	0.4(N4)	0.5(N5)
Small(S)	3	3	3	3
Medium(M)	3	3	3	3
Large(L)	3	3	3	3

Note : 1 in = 25.4 mm, 1 pound = 4.448 Newton

All specimens, both beams and cylinders, were cured in a lime saturated water until one day before testing, when they were taken out to cut the notch, attach the clip gage holders and the beam mounted reference frame holders. The average compressive strength and average Young's modulus were 5720 psi and 3120 ksi, respectively.

The main object of the experimental program is to obtain the complete load vs. *CMOD* and load vs. load point deflection curves then, to use them to analyze the material behavior for a variety of testing configurations. Table 1 summarizes the testing program. The parameter a/d is the ratio of the notch depth, a, to the depth of the beam, d. The three beam sizes and the four a/d ratios were selected to investigate how the beam size and the notch depth affects the fracture parameters.

All samples were tested on an MTS system 442 closed-loop servo controlled hydraulic testing machine. The closed-loop system enabled the use of *CMOD* control under which the *CMOD* was increased at a rate of 0.002 inch per minute. This mode of control produces a controlled failure of the sample allowing all parameters of interest to be measured. Raw data were recorded using a PC based data acquisition and control board running the Unkelscope data acquisition program sampling at 2 Hz.

Before testing the exact beam dimensions, notch depth and span were measured and recorded. Samples were installed on a flexural testing stand as shown in Fig. 3. The sample supports were semicircles. The load was applied through a swiveling arrangement that adjusted for sample irregularities.

Four measurements were made and electronically recorded by the data acquisition system. The load was measured by a 5,000 pound load cell, calibrated just prior to the start of the testing, attached to the MTS piston. Two measurements of the load-line deflection were made. The first, LVDT1, was made using a linear variable differential transformer (LVDT), resolving 0.05 inch into ten volts, measuring between the beam and a reference frame attached at the level of one half the unnotched depth, as seen in Fig. 3. The reference frame was hinged above one support and free to move laterally above the other. The second

measurement, LVDT2, was a conventional measurement, made also using an LVDT with the same range characteristics of LVDT1, between the beam and a fixture attached to the test stand. The last measurement was of the *CMOD*, made with an MTS clip-on gage which resolved 0.02 inch into ten volts.

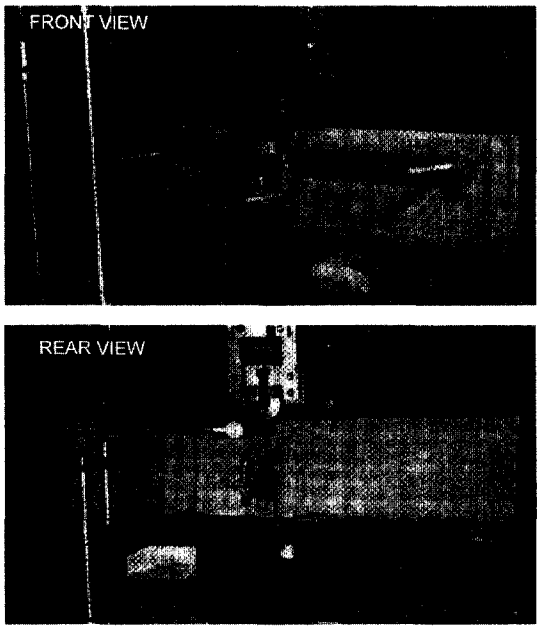

Fig. 3 Testing setup

4. Result and discussions

4.1 Extraneous deformations

The experimental results allow for a direct comparison of two methods of measuring the beam deflection. The results indicate that measurements made from a reference off the beam tend to overstate the actual deflection. Fig. 4 shows some typical load deflection curves. Testing results show that for all beam sizes and all notch conditions the deflection measured with reference off the beam (LPD2) measured with LVDT2 is greater than deflections measured with reference to the neutral axis of the beam (LPD1) measured with LVDT1. This effect, which has heretofore been believed to be negligible, is primarily due to crushing at the supports. Unfortunately, the magnitude of the extraneous deformation is of the same order as the actual beam deflection. The failure to consider the extraneous deformations has led to some misconceptions about the behavior of concrete samples. Fig. 5 shows the ratio of LPD2 to LPD1 at the peak load. In all cases, LVDT2 always

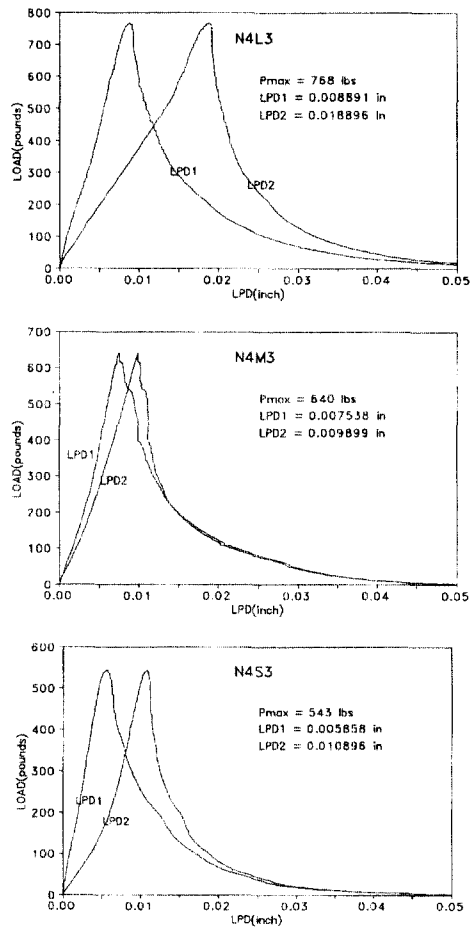

Fig. 4 Load-deflection relationship (1 lb = 4.448 N, 1 in = 25.4 mm)

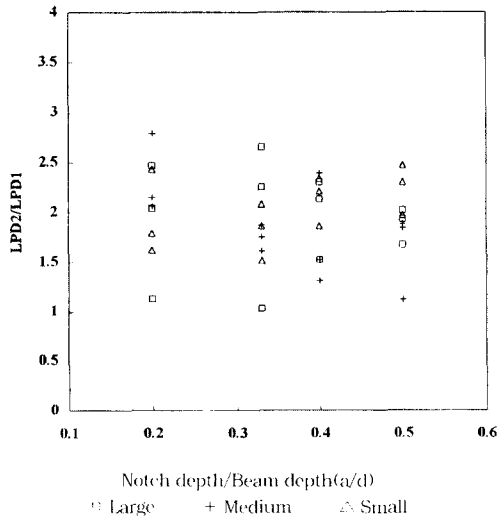

Fig. 5 The ratio LPD2 to LPD1 at the peak load

indicates a larger deformation than LVDT1 so the ratio always exceeds 1.0, which shows that LPD2 always includes some degree of settlement. It can also be noted that after the peak load no further crushing occurs. A calculation of fracture energy, G_F based upon this overstated deflection will give an inflated value. For accurate measurement of beam deflections a reference attached to the beam, of the sort used in these experiments, should be used.

Until the current study the *CMOD* has primarily been used to control the specimen loading rate. However, since the *CMOD* is relatively unaffected by support settlements it was thought that it might be a more reliable fracture parameter. Fig. 6 is a typical load-*CMOD* curve, it has a strong resemblance to typical load-deflection curves. Typical deflection-*CMOD* curves are shown in Fig. 7. The lower curve shows the LVDT2 deflection vs. *CMOD* and apparently there is no clear relationship between the deflection and the *CMOD*. Strikingly, the LVDT1 deflection vs. *CMOD* shows a simple bilinear relationship.

4.2 Bilinear deflection-CMOD relationship

The deflection-*CMOD* relationship, shown in Fig. 7 is observed to be bilinear. The first linear part, S_1, shows the deflection-*CMOD* relationship in the linear elastic region. As the microcracked process zone develops the slope gradually changes until the peak load is reached. At this point the process zone is completely developed and cracking begins. The second linear portion, S_2, is sustained as the crack grows until complete failure. Since nonlinearity of concrete is mainly a contribution of the microcracked zone, the size of the process zone in front of the crack tip remains fully developed and shifts forward as the macrocrack grows. It can be noted on Fig. 7 that if the LVDT2 deflection (LPD2), which includes the extraneous deformations, is considered this relationship is not at all apparent.

S_2 is the slope of the deflection-*CMOD* curve as the crack propagate through the specimen. The values of S_2 for the concrete used in this study are shown in Fig. 8. It can be seen from Fig. 8 that the values, which average 0.8720, are very consistent. This

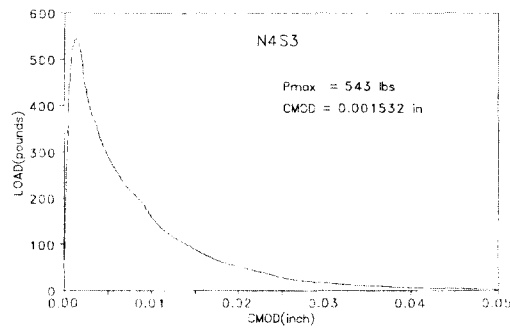

Fig. 6 Typical load-*CMOD* curve (1 lb = 4.448 N, 1 in = 25.4 mm)

indicates that S_2 is a material property in the same way that G_F is a material property.

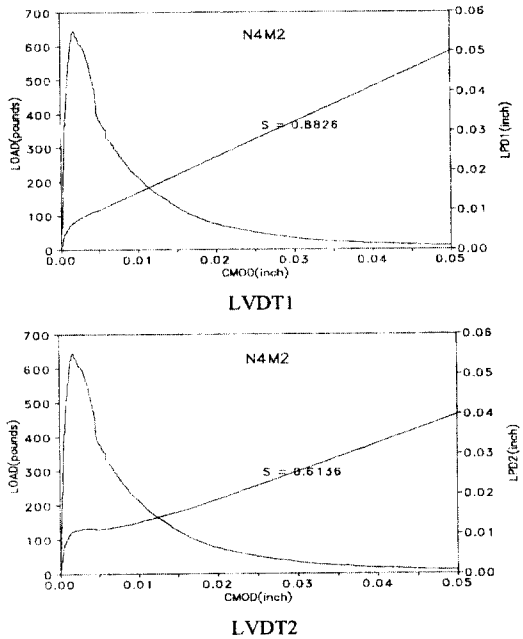

Fig. 7 Load-*CMOD*-deflection relationship (1 lb = 4.448 N, 1 in = 25.4 mm)

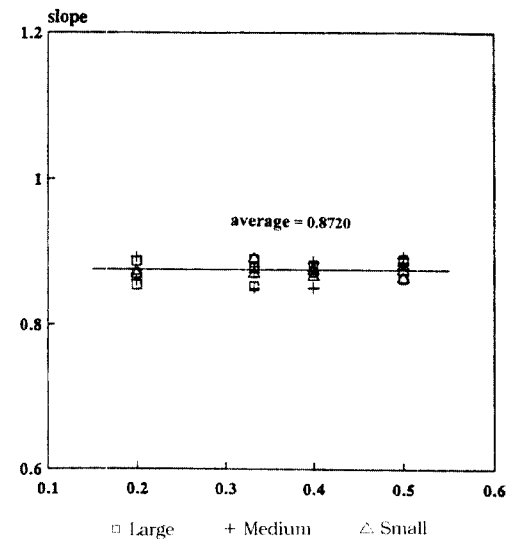

Fig. 8 Observed values of S_2

The fracture energy is usually taken as the area under the load-deflection curve. However, there have been many discrepancies for determining the fracture energy for cementitious composites, now thought to have been due, in large part, to the difficulties encountered making exact measurements of the load-line deflection. These problems can be eliminated using the bilinear concept because the *CMOD* value is used to calculate the fracture energy. The fracture energy is computed using the following expression:

$$G_F = \int_0^{\delta_0} P d\delta = C \int_0^{\delta_0} P dCMOD \qquad (19)$$

where C is S_1 in the elastic range and S_2 in the post-peak region as long as S_1 and S_2 are constants.

4.3 Pe/Pmax limit

The ratio of load at the elastic limit, Pe, to the maximum load, Pmax, indicates the extent of the fracture process zone. The assumption of the current fracture mechanics theory, as it applies to concrete, is that up until the proportional limit there is no process zone or microcracking. After the proportional limit the process zone gradually develops until it reaches its full extent when the peak load is reached and the macrocrack begins to propagate. A small ratio of Pe/Pmax would indicate a relatively larger process zone than a larger ratio for the same configuration. Values of Pe/Pmax, calculated using the *CMOD* - deflection relationship, plotted against a/d for all samples are shown in Fig. 9. This figure shows that as the notch depth increases the ratio of Pe/Pmax increases until it exceeds 1.0.

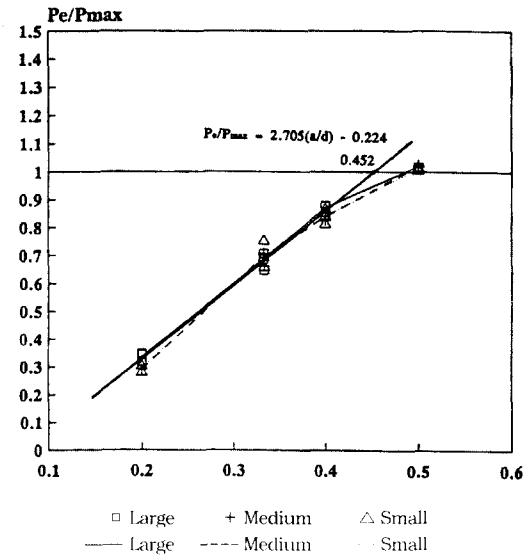

Fig. 9 Relationship between Pe/Pmax and *a/d*

Conceptually, the value of Pe/Pmax can not be greater than 1.0. However, when a/d equal to 0.5 Pe/Pmax was found to exceed 1.0. The interpretation of this result is that at this notch size the process zone for the beam reaches the confinement of the compression zone before being fully developed. Therefore, the zone can develop no further so cracking starts relatively earlier than for other notch sizes resulting in a lower peak load and lower fracture energy.

RILEM's committee on fracture toughness of concrete recommends that when measuring the fracture energy of concrete using three-point bend notched beams a/d should be 0.5. Presently, most researchers follow these recommendations. The results of this study indicate that there may be problems with this recommendation and that the recommendation for a/d should be changed. An a/d less than 0.4, which is a/d when Pe/Pmax is appropriately 1.0 should be used.

4.4 Fracture energy

Fracture energy is a very important parameter used in studying the properties of concrete. It is the amount of energy required to extend a crack a unit area through the material. If the fracture energy is known then the behavior of a structure can be predicted more accurately. Fig. 10 shows G_F calculated based on the LVDT2 measurements. The value of G_F is seen to be widely scattered, an effect not uncommon when many measurements of the same sort are made. Fig. 11 shows G_F calculated based on the bilinear concept. The value is seen to be essentially constant until it drops when a/d equals 0.5, for the reasons discussed above in the section on Pe/Pmax. Again, since the fracture energy is one of the parameters sought when testing using RILEM recommendations, the current recommendation of 0.5 needs to be changed.

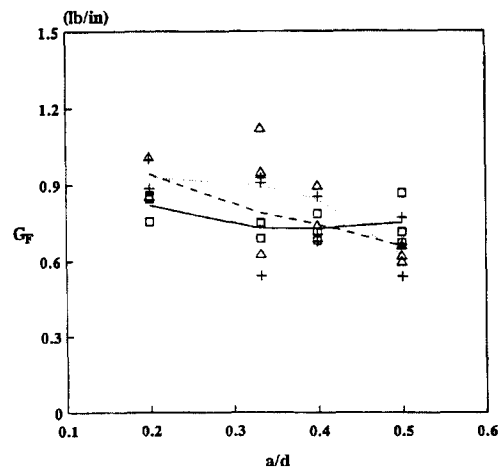

Fig. 10 Fracture energy calculated based on deflection measurement(1 lb/in = 175.13 N/m)

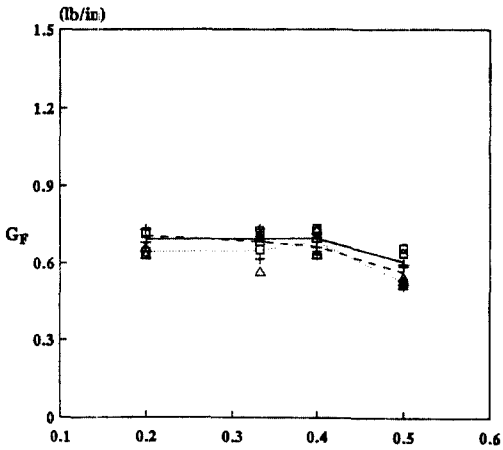

Fig. 11 Fracture energy calculated based on bilinear concept (1 lb/in = 175.13 N/m)

5. Conclusions

Based on the results obtained through this study, following conclusions can be drawn:

1) Traditional methods for measuring load-line deflections in beams, which are commonly measured with respect to the base of the testing machine, contain extraneous measurements that are of the same order of magnitude as the actual deflection of the beam. These extraneous measurements are mostly the result of support crushing, which can be eliminated by measuring the beam deflections with reference to its neutral axis using a reference frame attached to the beam. In this study, a new test setup for measuring the load-line deflection in a notched beam test is proposed.

2) When proper measurements of a beam's deflection are made, a bilinear relationship between the *CMOD* and the deflection is found to exist. This bilinear relationship serves as the critical tool to relate the *CMOD* to the fracture energy of the notched beam.

3) The deflection-*CMOD* relationships in the pre and post peak regions, S_1 and S_2 respectively, are material properties.

4) To avoid using the complicated testing setup required for properly measuring the load-line deflection of beams, the *CMOD*, which is unaffected by support crushing or other extraneous measurements, is a more reliable parameter for predicting the fracture properties of concrete. Use of the load-*CMOD* relationship along with the proposed S_1 and S_2 relationships could lead to a new testing standard for measuring fracture energy of concrete.

5) Analysis of Pe/Pmax for various notch depths indicates the progression of the process zone into the region of effective confinement caused by the compression zone of the beam. The analysis further indicates the need to change the current RILEM recommended a/d of 0.5 to a value of 0.4 to avoid this effect and improve measurement of fracture energy.

References

1. Hawkins, N. M., "The Role for Fracture Mechanics in Conventional Reinforced Concrete Design," Proceedings of the NATO Advanced Research Workshop on Application of Fracture Mechanics to Cementitious Materials, Northwestern University, Evanston, Illinois, USA, 1984, pp.639-666.
2. Elfgren, L., "Application of Fracture Mechanics to Concrete Structures," Proceedings of International Workshop on the Fracture Toughness and Fracture Energy, Sendai, Japan, 1988, pp.575-590.
3. Darwin, D., S. L. McCabe, C. J. Brown and C. Schumm, "Fracture Analysis of Steel-Concrete Bond," Proceedings of the US-Europe Workshop on Fracture and Damage in Quasibrittle Structures, Prague, Czech Republic, 1994, pp.549-

556.

4. RILEM Draft Recommendation, "Determination of the Fracture Energy of Mortar and Concrete by means of Three-Point Bend Tests on Notched Beams," Materials and Structures, Vol.18, No 106, 1985, pp.285-296.
5. Hillerborg, A., "Results of Three Comparative Test Series for Determining the Fracture Energy G_F of Concrete," Materials and Structures, Vol. 18, No. 107, 1985, pp.407-413.
6. Gopalaratnam, V. S., S. P. Shah, G. B. Batson, M. E. Criswell, V. Ramakrishnan, and M. Wecharatana, "Fracture Toughness of Fiber Reinforced Concrete," ACI Materials Journal, Vol. 88, No. 4, 1991, pp.339-353.
7. Tada, H., P. C. Paris and G. R. Irwin, The Stress Analysis of Cracks Handbook, Del Research Corporation, Hellertown, Pennsylvania, 1976.
8. ASTM E399-83, "Standard Method of Test for Plane-Strain Fracture Toughness of Metallic Materials," American Society for Testing and Materials, N.Y. N.Y., 1983.

(접수일자 : 1996. 12. 11)